©2022 Published in 6th International Symposium on Natural Hazards and Disaster Management
21-23 October 2022 (ISHAD2022 Bursa - Turkey)
https://doi.org/10.33793/acperpro.XXXX

ACADEMIC PLATFORM

The September 26, 2019 Silivri Earthquake (M_W=5.6), NW Türkiye

*1,2Murat Utkucu, [1]Fatih Uzunca, [3]Yelçin Utkucu, [4]Hatice Durmuş, [1]Serap Kızılbuğa
[1]*Sakarya University Engineering Faculty Department of Geophysics 54187, Serdivan, SAKARYA*
[2]*Sakarya University, Disaster Management Application and Research Center, Serdivan, SAKARYA*
[3]*TOBB MATL High School, Serdivan, Sakarya*
[4]*Kütahya Dumlupınar University Engineering Faculty Department of Geological Engineering, 43100, KÜTAHYA*

Abstract:

The September 26, 2019 Silivri earthquake (M_W=5.6-5.8) occurred along the North Anatolian Fault Zone segments extending beneath the Marmara Sea. In the present study the teleseismic *P* waveforms and 20-year long background seismicity of the earthquake (M_W=5.6-5.8) have been analyzed. Point-source inversion of the teleseismic *P* waveforms revealed that the earthquake was due to oblique faulting and released a seismic moment of 3.2 x 10^{17} Nm (M_W=5.6). The frequency-magnitude distributions (FMDs) for the background seismicity have been calculated after the 1999 İzmit earthquake. The considerable decrease of *b*-value of the FMD before the 2019 Silivri earthquake has been interpreted as stress increase along the fault segments.

Key words: The North Anatolian Fault Zone; The 26 September 2019 Silivri earthquake, *b*-value

1. Introduction

The Marmara Region has been characterized by high seismic activity with tens of devastating large earthquakes in the history (Figure 1) [1, 2, 3]. The high seismic activity has been generated by the North Anatolian Fault Zone (NAFZ) which extends as three main fault strands, the Northern, Middle and Southern strands [4, 5] (Figure 1). As seen from Figure 1 the Northern fault strand has generated most of the large earthquakes. This fact indicates that the Northern fault strand has played major role in accommodating the deformation resulting from the regional plate kinematics, in accordance with GPS studies [6, 7].

The fault segments of the Northern Strand have been indicated to be a seismic gap after the occurrence of the 1999 İzmit earthquake (M_w=7.5) (Figure 1) [8, 9, 10]. The largest city of Türkiye, İstanbul is located close to the seismic gap causing a high seismic risk. The September 26, 2019 Silivri earthquake (M_W=5.6-5.8) occurred within the seismic gap along the Northern Strand (KOERI 2019; AFAD 2019; MTA 2019) (Figure 1) and caused slight structural damage and big fear among the population. In the present study teleseismic waveforms and seismicity around the earthquake will be analyzed in order to have an idea about seismotectonic meaning of the earthquake.

**Corresponding author: Murat Utkucu, Address: Sakarya University Engineering Faculty Department of Geophysics 54187, Serdivan, SAKARYA, TÜRKİYE. E-mail address: mutkucu@sakarya.edu.tr

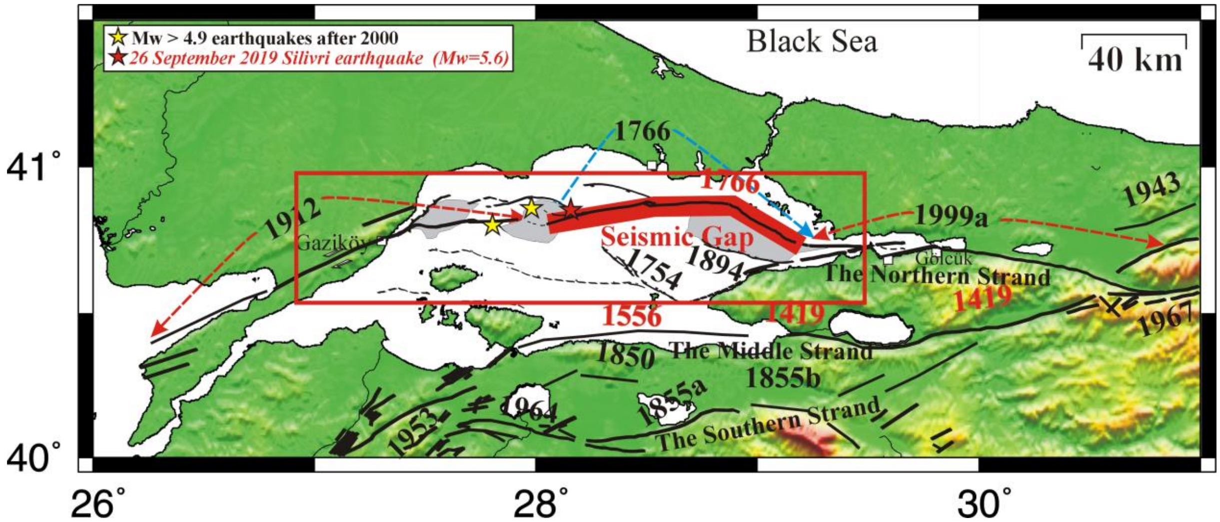

Figure 1. The map demonstrating extent of the North Anatolian Fault Zone (NAFZ) and large historical earthquakes in the Marmara Region. The faults are compiled from Barka and Kadinsky-Cade (1988), Armijo et al., (2002), and Emre et al. (2013) [4, 11, 5] and the historical seismicity is taken from, Ambraseys (2002, 2009), [12, 13]. The large rectangle encloses the areas in which the seismicity shown in Figures 3a and 4a have been recorded. Red thick line indicates fault segments that produced no large earthquake for the last hundred years along the Northern Strand and considered as seismic gap.

2. Teleseismic Source Process

Teleseismic *P* waveforms of the 2019 Silivri earthquake recorded at 15 stations are inverted to investigate the source process and to obtain the source parameters. Point-source inversion methodology developed by Kikuchi and Kanamori (1991) is applied to the teleseismic *P* displacement waveforms, lengths of which are taken as 16 s [14]. The earthquake rupture has been approximated by a vertical grid of 5x5 point-sources along the strike and dip, respectively (Figure 2).

The waveforms are satisfactorily fitted using single point-source located at the hypocentral depth (10 km). The results of the inversion are depicted in Figure 2 and calculated source parameters are listed in Table 1. Both hypocentral and source parameters of the earthquake suggest that the earthquake was due to oblique faulting with strike-slip and reverse faulting components. Adding relocation of the earthquake together with the detailed fault mapping suggest that the earthquake occurred on a secondary fault extending north of the main fault trace [15, 16, 17, 18]. The solution demonstrated in Figure 2 corresponds to a seismic moment of 3.2 x 10^{17} Nm (M_W=5.6).

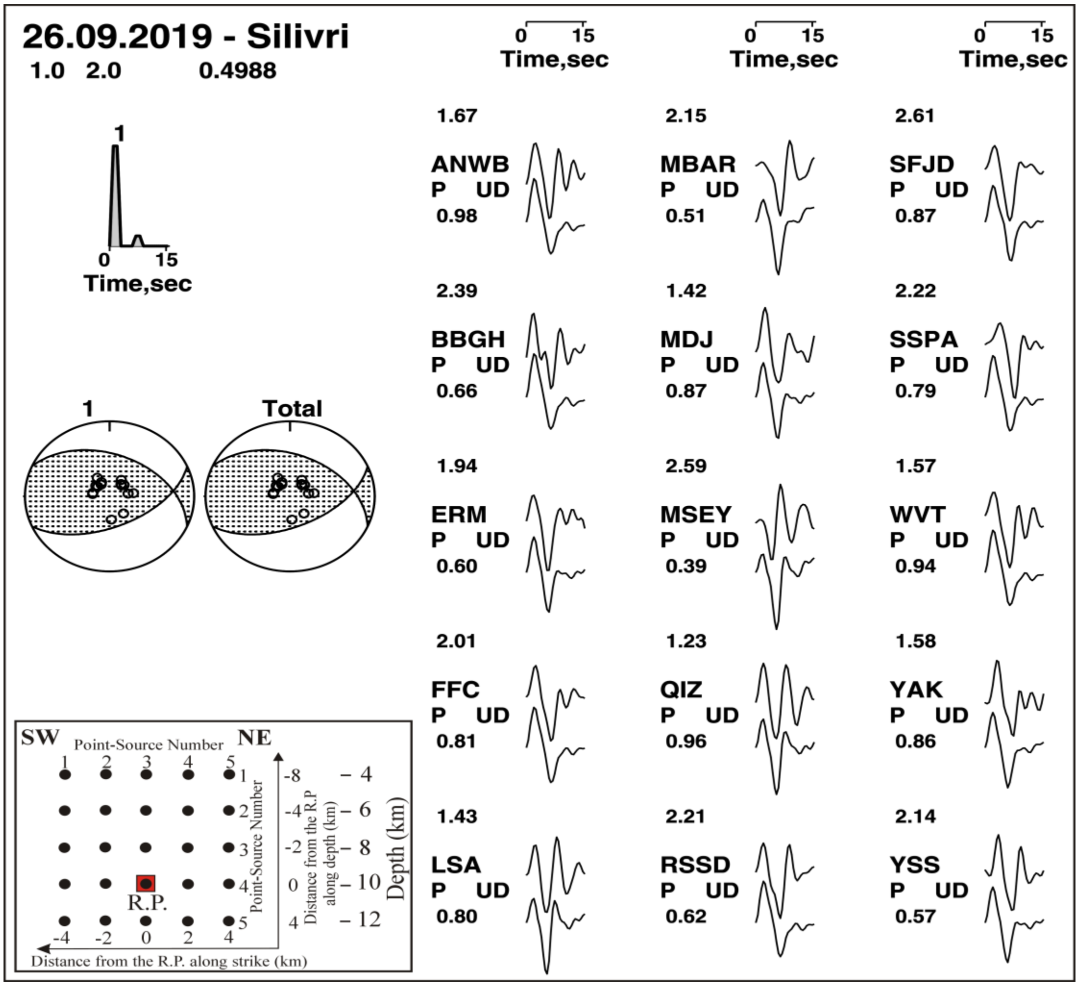

Figure 2. Teleseismic point-source analysis results of the September 26, 2019 Silivri earthquake. (*Left*) Source-time function, source mechanism and retrieved location of the single point-source. R.P. stands for the reference point which is taken as the hypocentral location in the analysis. (R*ight*) Comparison of the observed waveforms (top) with synthetic waveforms (bottom) calculated for the point-source mechanism and location shown in the left.

Table 1. Source parameters of the 26 September 2019 Silivri earthquake

	Longitude (°)	Latitude (°)	Depth (km)	Magnitude	Strike (°)	Dip (°)	Rake (°)	Seismic Moment (10^{18} N m)
USGS	28.150	40.904	8	Mw=5.71	86	64	123	0.4575
NEIC					210	42	42	
This					66	54	59	0.32
Study					294	44	128	

USGS= United States Geological Survey; NEIC= National Earthquake Information Center

3. Seismicity Analysis

Gutenberg-Richter relation of the earthquake occurrences defines frequency-magnitude distribution (FMD) of earthquakes [19] and is given:

$$\log_{10} N = a - bM \tag{1}$$

where N represents cumulative number of earthquakes of size M and larger, and a and b are constant parameters. The parameter b-value is an important seismotectonic parameter which has been pointed out to be inversely related to the crustal stresses [20, 21]. In order to calculate a and b-values the Weigted Least Square method is utilized [22]. Following determination of the FMD relation from the seismicity recurrence time (T_r) and occurrence possibility of an earthquake (R) of targeted magnitude (M_{targ}) in a defined future (t) can be calculated by equations below

$$T_r = \frac{\Delta T}{10^{(a - bM_{targ})}} \tag{2}$$

$$R = 1 - e^{-N(Mtarg)t} \tag{3}$$

$$N(M_{targ}) = 10^{(a-bMtarg)} \tag{4}$$

where ΔT is the recording period of the seismicity [21, 23]. $N(M_{targ})$ corresponds annual number of occurrences of the targeted event. The *ZMAP* software is utilized for defining the FMD for the selected seismicity data [24]. Recurrence times and seismic risk are calculated manually.

A homogenized catalogue that covers the time period from 1900 to October 2018 and is based on moment magnitude has been used in the seismicity analysis [3]. Kandilli Observatory and Earthquake Research Institute (KOERI) catalogue has been used to extend catalogue period until July 2020.

The seismicity after the 1999 İzmit earthquake and along the Northern Strand beneath the Marmara Sea. After declustering and initial checking of the catalogue the seismicity having magnitude above 2.8 is decided to be used in the seismicity because the catalogue is relatively homogeneous after that time for that magnitude of completeness analysis. Calculated magnitude of completeness time variations for the declustered seismicity and cumulative numbers are shown in Figure 3a and 3b, respectively. Cumulative numbers of the declustered Mc≥2.8 seismicity is depicted in Figure 3c. Notice how the seismicity data becomes more homogeneous after leaving only M≥2.8 earthquakes in the catalogue. The epicentral distribution of the earthquakes in this catalogue is demonstrated Figure 4 along with the FMD.

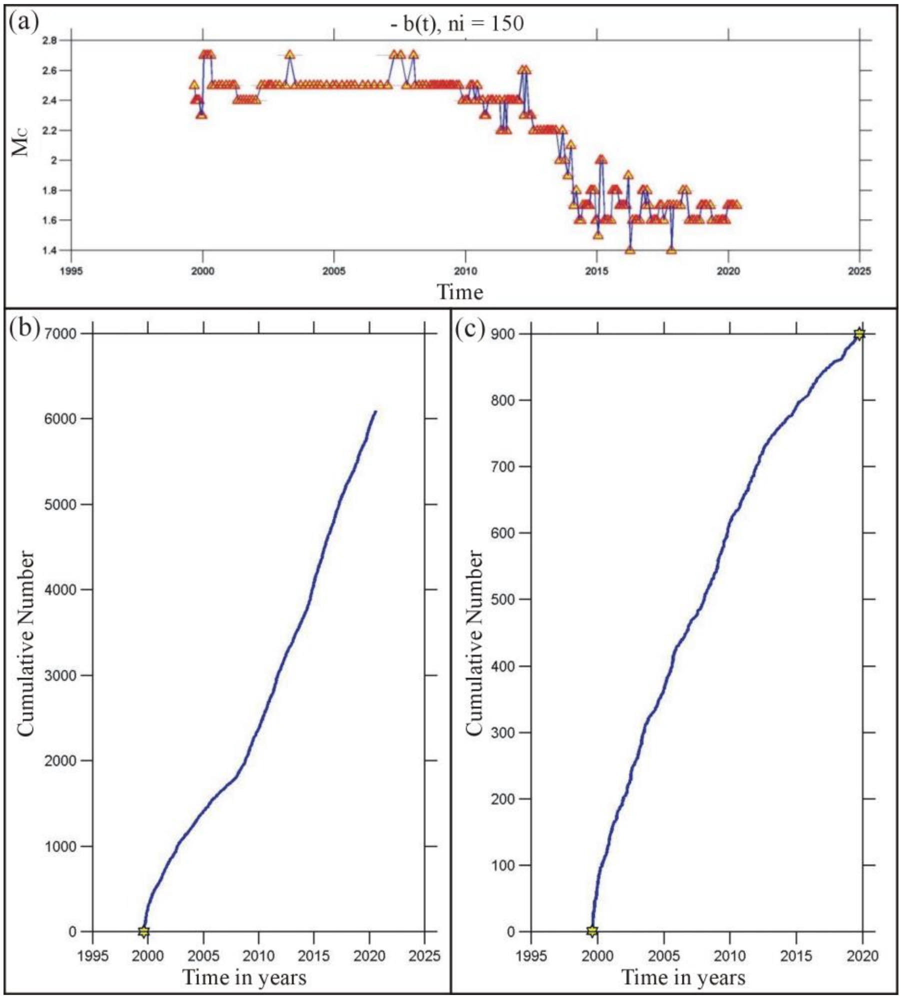

Figure 3 (a) The calculated magnitude of completeness (Mc) time variations for declustered, all-magnitude seismicity along the Northern Strand after 1999 İzmit earthquake and (b) cumulative numbers of the seismicity shown. (c) Cumulative numbers of the seismicity for Mc≥2.8.

4. Discussion

Either source mechanism solution obtained in the study (Figure 2) coincides with that the 2019 Silivri earthquake occurred along a secondary fault associated with a fault jog in the Central Basin of the Marmara Sea. In order to investigate if the background seismicity present a clue for occurrence of the 2019 Silivri earthquake the FMDs are estimated in 5-year time windows after the 1999 İzmit earthquake. Though *b*-value is 1.06 for the 20 year period (Figure 4b) considerable variations of *b*-value is estimated for shorter time periods. Between 2004 and 2009 *b*-value increased to 1.17 as compared with 5-year period just after the 1999 İzmit earthquake. Then it has gradually dropped 1.03 and 0.91 in the time intervals of 2009-2014 and 2014-2019. The significant drop in *b*-value suggests rise of crustal stresses along the fault segments lying beneath the Marmara Sea. This provides a reasonable clue for the occurrence of the 2019 Silivri earthquake.

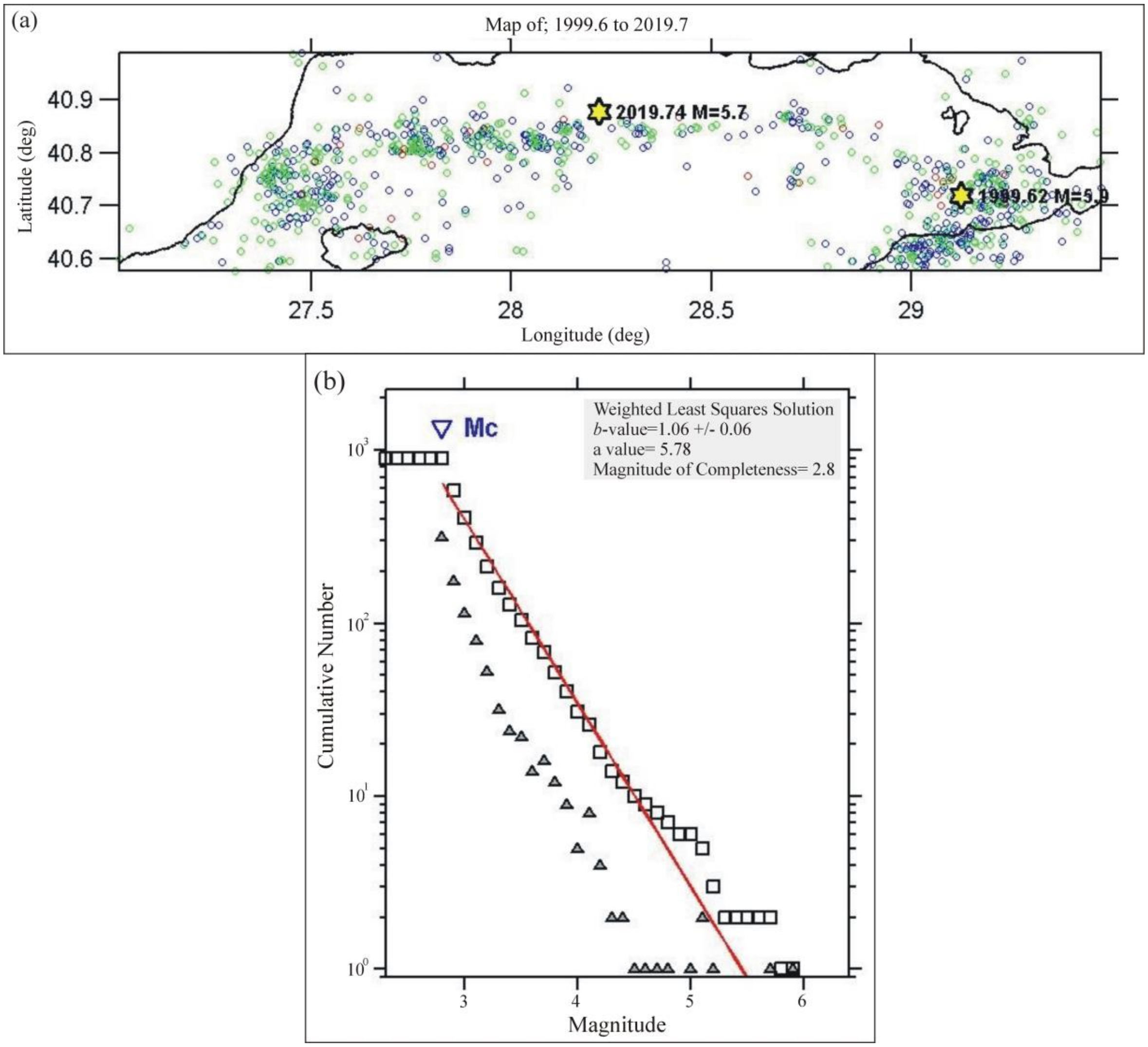

Figure 4 (a) Epicentral distribution of declustered Mc≥2.8 seismicity and (b) its estimated Frequency-Magnitude distribution.

Conclusions

In the present study teleseismic P waveforms of the September 26, 2019 Silivri have been inverted for the source process and the background seismicity around the earthquake has been analyzed. The waveforms are fitted using single point-source located at the hypocentral depth (10 km) and calculated source parameters suggest that the earthquake was due to oblique faulting. The earthquake released a seismic moment of 3.2 x 10^{17} Nm (M_W=5.6). The frequency-magnitude distributions (FMDs) for the background seismicity have been calculated in 5-year long time windows after the 1999 İzmit earthquake. The considerable decrease of *b*-value of the FMD for the time interval of 2014-2019 has been interpreted as stress increase along the fault segments which provides a reasonable clue for the occurrence of the 2019 Silivri earthquake.

Acknowledgements

This study was funded by The Scientific and Technical Research Council of Türkiye (TÜBİTAK) (project number: 121Y271).

References

[1] Ambraseys N.N, Finkel C.F. The Saros-Marmara earthquake of 9 August 1912. Earthquake Eng. and Struct. Dyn 1987; 5; 189-211.

[2] Kalafat D, Günes Y, Kara M, Deniz P, Kekovalı K, Kuleli, et all. A revised and extended earthquake catalogue for Turkey since 1900 (M4.0). Boğaziçi University, Kandilli Rasathanesi ve Deprem Araştırma Enstitüsü, Bebek-İstanbul 2007; 2007.3; 553.

[3] Tan A. A homogeneous earthquake catalogue for Turkey. Nat. Hazards Earth Syst. Sci. 2021; 21; 2059–2073.

[4] Barka A, Kadinsky-Cade K. Strike-slip fault geometry in Turkey and its influence on earthquake activity. Tectonics 1988; 7; 663-684.

[5] Emre Ö, Duman T Y, Özalp S, Elmacı H, Olgun Ş, Şaroğlu F. Active fault map of Turkey with explanatory text, General Directorate of Mineral Research and Exploration Special Publication Series 2013; 30.

[6] Flerit F, Armijo R, King G.C.P, Meyer B, Barka A. Slip partitioning in the Sea of Marmara pull-apart determined from GPS velocity vectors. Geophys. J. Int. 2003; 154; 1-7.

[7] Reilinger R, McClusky S, Vernant P, Lawrence S, Ergİntav S, Cakmak R, et all. GPS constraints on continental deformation in the Africa-Arabia-Eurasia continental collision zone and implications for the dynamics of plate interactions. J. Geophys. Res. 2006; 111.

[8] Parsons T, Toda S, Stein R.S, Barka A, Dieterich J.H. Heightened odds of large Earthquakes near İstanbul: An interaction-based probability calculation. Science 2000; 288; 661-665.

[9] Ferrari H, Barka A, Jacques E, Nalbant S, Meyer B, Armijo R, Paul et all. Seismic hazard in the Marmara Sea region following the 17 August 1999 Izmit earthquake. Nature 2000; 404; 262-27.

[10] Utkucu M, Kanbur Z, Alptekin Ö, Sünbül F. Seismic behavior of the North Anatolian Fault beneath the Sea of Marmara (NW Turkey): implications for earthquake recurrence times and future seismic hazard. *Natural Hazards* 2009; *50*(1); 45-71.

[11] Armijo T, Meyer B, Navarro S, King G, Barka A. Asymetric slip partitioning in the Sea of Marmara pull-apart: a clue to propagation processes of the North Anatolian Fault. Terra Nova 2002; 14; 80-86.

[12] Ambraseys N. The seismic activity of the Marmara Sea Region over the last 2000 years. Bull. Seism. Soc. America 2002; 92; 1-18.

[13] Ambseys N.N. Earthquakes in the Mediterranean and Middle East: a multidisciplinary study of seismicity up to 1900. Cambridge University Press. 2009; ISBN: 978-0-521-87292-8.

[14] Kikuchi M, Hiroo K. Inversion of complex body waves-III. Bulletin of the Seismological Society of America 1991; 81(6); 2335-2350.

[15] Armijo T, et al. Submarine fault scarps in the Sea of Marmara pull-apart (North Anatolian Fault): Implications for seismic hazard in İstanbul. Geochem. Geophys. Geosyst 2005; 6; doi:10.1029/2004GC000896.

[16] Burnard, P, Bourlange P, Henry L, Geli, M. D, Tryon B, et al. Constraints on fluid origins and migrate on velocities along the Marmara Main Fault (Sea of Marmara, Turkey) using helium isotopes. Earth and Planetary Science Letters 2012;341-344; 68-78.

[17] Batsi E, Anthony L, Jean-Baptiste T, Frauke K, Vincent R, Shane M. An Alternative View of the Microseismicity along the Western Main Marmara Fault. Bulletin of the Seismological Society of America 2018;108; 2650-2674.

[18] Yamamoto Y, Kalafat D, Pinar A, Narumi T, Çoşkun Z, Polat R, et al. Fault geometry beneath the western and Central Marmara Sea, Turkey, based on ocean bottom seismographic observations: Implications for future large earthquakes. Tectonophysics 2020; 791.

[19] Gutenberg R, Richter C. F. Frequency of earthquakes in California. Bull. Seismol. Soc. Am 1944; 34; 185-188.

[20] Scholz C.H. Experimental Study of the Fracturing Process in Brittle Rock. Journal of Geophysical Research 1968; 73.4; 1447-1454.

[21] Wiemer S, Wyss M. Mapping the frequency-magnitude distribution in asperities: an improved technique to calculate recurrence times Journal Geophys. Resarch 1997;102; 15115-15128.

[22] Menke W. Geophysical Data Analysis: Discrete Inverse Theory. International Geophysics Series 1989; 45; ISBN -0-12-490921-3, 1989.

[23] Öncel A.O, Wyss M. The major asperities of the 1999 M_W=7.4 İzmit earthquake defined by the microseismicity of the two decades before it. Geophys. Journal Int. *2000;* 143; 501-506.

[24] Wiemer S. A software package to analyze seismicity: ZMAP. Seismological Research Letters 2001; 72(3); 373–382.